



Metal catalysts supported on activated carbon fibers for removal of polycyclic aromatic hydrocarbons from incineration flue gas

Chiou-Liang Lin^a, Yu-Hsiang Cheng^b, Zhen-Shu Liu^{b,*}, Jian-Yuan Chen^b

^a Department of Civil and Environmental Engineering, National University of Kaohsiung, Kaohsiung 811, Taiwan, ROC

^b Department of Safety, Health and Environmental Engineering, Ming-Chi University of Technology, Taishan District, New Taipei City 243, Taiwan, ROC

ARTICLE INFO

Article history:

Received 31 March 2011

Received in revised form

21 September 2011

Accepted 22 September 2011

Available online 5 October 2011

Keywords:

Adsorption

Catalytic oxidation

Activated carbon fiber

PAHs

Incineration flue gas

ABSTRACT

The aim of this research was to use metal catalysts supported on activated carbon fibers (ACFs) to remove 16 species of polycyclic aromatic hydrocarbons (PAHs) from incineration flue gas. We tested three different metal loadings (0.11 wt%, 0.29 wt%, and 0.34 wt%) and metals (Pt, Pd, and Cu), and two different pretreatment solutions (HNO₃ and NaOH). The results demonstrated that the ACF-supported metal catalysts removed the PAHs through adsorption and catalysis. Among the three metals, Pt was most easily adsorbed on the ACFs and was the most active in oxidation of PAHs. The mesopore volumes and density of new functional groups increased significantly after the ACFs were pretreated with either solutions, and this increased the measured metal loading in HNO₃-0.48% Pd/ACFs and NaOH-0.52% Pd/ACFs. These data confirm that improved PAH removal can be achieved with HNO₃-0.48% Pd/ACFs and NaOH-0.52% Pd/ACFs.

© 2011 Elsevier B.V. All rights reserved.

1. Introduction

Organic compounds released in waste incineration flue gas have received considerable attention due to their mutagenic and carcinogenic properties. Among these organic compounds, the U.S. Environmental Protection Agency (USEPA) lists 16 polycyclic aromatic hydrocarbon (PAH) species in particular as priority pollutants. Our previous study indicated that a conventional air pollution control device (APCD) comprising a spray dryer integrated with a fabric filter can achieve a removal efficiency of only 40% for PAHs [1]. To devise an improved method, we tested the use of activated carbon fibers (ACFs) as adsorbents and found that although the overall removal efficiency of the PAHs increased up to 90%, the removal efficiencies for some PAH species were negative [2]. Moreover, additional processes are necessary to deal with the adsorbed PAHs. As an alternative approach, we investigated the efficiency of removal by oxidation with metal catalysts (Pt, Pd, and Cu) supported on ACFs for the 16 PAH species from incineration flue gas.

Catalytic oxidation of organic compounds to carbon dioxide and water is most appealing owing to its low reaction temperature and high removal efficiency which depends mainly on the catalyst support, nature of the active site, and the preparation method. The most common supports used in catalytic oxidation of organic compounds

are Al₂O₃, zeolites, and granular activated carbons (GACs) [3–6]. However, the use of other materials such as ACFs has also been studied in a minor extension [7–9]. Compared with the common support materials mentioned above, ACFs present a much larger specific surface area and have a more uniform micropore structure, faster adsorption and desorption rates, a faster equilibrium rate, and high fluid permeability [8–11].

Two groups of catalysts used widely for the oxidation of organic compounds are noble metals (Pt, Pd, Rh, and Au) and base metals (Mn, Co, Cu, Fe, and Ni). The former possess higher catalytic activity and selectivity for the oxidation of organic compounds at low temperature [12]. However, because of their much higher cost, the latter have been more widely investigated for oxidation of organic compounds [13–15]. Kim investigated the catalytic activity of Cu, Mn, Fe, V, Mo, Co, Ni, and Zn supported on γ -Al₂O₃ in the oxidation of benzene, toluene, and xylene. The most promising was found to be Cu/ γ -Al₂O₃ on the basis of its activity [14]. Thus, Pt, Pd, and Cu supported on ACFs were studied in this research.

Many studies on the use of activated carbons (ACs) as supports have found that the catalytic properties of metals are influenced by the physical and chemical properties of the supports. The chemical characteristics of the supports can be modified by different pretreatments, including functionalization and oxidation treatments [6,16–18]. Wu et al. investigated catalytic oxidation of BTX using Pt supported on ACs that were heated to 400 or 800 °C under N₂ flow and washed with HF acid. Their experimental results showed that the high-temperature pretreatment of the AC supports was

* Corresponding author. Tel.: +886 2 29089899x4698; fax: +886 2 29041914.
E-mail address: zslu@mail.mcut.edu.tw (Z.-S. Liu).

effective in increasing the activity of the catalyst [6]. Hermans et al. functionalized AC supports with HNO_3 or H_2O_2 solutions and reported that the catalytic activity could be correlated with the initial carbon acidity and Pd dispersion, which were improved in the HNO_3 -modified supports [17].

Metal catalysts supported on ACFs exhibit higher catalytic oxidation efficiency than those supported on GACs. Our earlier studies showed that common APCDs were very inefficient in the removal of PAHs [1]. Furthermore, the control of organic compounds with ACFs was carried out only using laboratory-scale rings, and the simultaneous removal of all 16 PAH species has rarely been examined. In this study we therefore set out to test the effectiveness of the ACF-supported metal catalysts in the removal of all 16 PAH species from flue gas from a fluidized-bed incinerator to simulate practical conditions. We tested three different metal loadings (0.11 wt%, 0.29 wt%, and 0.34 wt%), three metals (Pt, Pd, and Cu), and two alternative pretreatment solutions (HNO_3 and NaOH).

2. Experimental

2.1. Preparation of ACF-supported catalysts

Commercial ACFs supplied by Taiwan Carbon Technology Co. Ltd., Taiwan, were used as the support. Before the preparation of the catalysts, the ACFs were cleaned with deionized water and then dried in an oven at 105°C for 24 h. To improve the physical and chemical properties of the ACFs, some were separately pretreated with HNO_3 and NaOH solution. The pretreatment was performed by immersing the ACFs in 1 M HNO_3 or NaOH solution for 48 h. Then, the ACFs pretreated with HNO_3 or NaOH were again washed with deionized water until the pH of the effluent water was around 7.0 and were then dried in the oven at 105°C for 24 h [19]. Afterwards, the ACFs were impregnated with the three metal species (Pt, Pd, and Cu) by the excess-solution impregnation method as follows:

The reagent of H_2PtCl_4 was mainly used as the metal precursor in previous studies [6,9]. Thus, the reagents of PtCl_4 , $\text{Pd}(\text{NO}_3)_2 \cdot 2\text{H}_2\text{O}$, and $\text{Cu}(\text{NO}_3)_2 \cdot 5/2\text{H}_2\text{O}$ were individually dissolved in deionized water to which the ACFs support was added. The solution was

Table 1
Code and compositions of various catalysts.

Catalyst	ACFs pretreatment	Metal loading (wt%)	
		Expected value	Actual value ^a
Original ACFs	–	–	–
0.11% Pd/ACFs	–	1.0	0.11
0.29% Pd/ACFs	–	1.5	0.29
0.34% Pd/ACFs	–	2.0	0.34
1.63% Pt/ACFs	–	2.0	1.63
0.53% Cu/ACFs	–	2.0	0.53
HNO_3 -0.48% Pd/ACFs	HNO_3	2.0	0.48
NaOH-0.52% Pd/ACFs	NaOH	2.0	0.52

^a Metal loading was determined by ICP.

stirred at 300 rpm in a water bath at room temperature for 1 h. Finally, the ACFs were filtered out and dried in an oven at 105°C for 24 h. Table 1 lists the nomenclature and compositions of the catalysts tested in this study.

2.2. Preparation of artificial feedstocks

To simulate actual flue gas, polypropylene (PP) was used as artificial incinerator feedstocks in this experiment. The feed materials were enclosed in a polyethylene (PE) bag. The total weight of each sample fed to the incinerator was 0.82 g.

2.3. Experimental apparatus and procedure

Fig. 1 illustrates the incineration system, which consisted of a laboratory-scale fluidized-bed incinerator connected to a reactor containing the ACF-supported catalysts. The height and inner diameter of the incinerator were 70 and 10 cm, respectively. The dimensionless velocity of inlet gas with respect to the umf at operating conditions was 2.5. The height and inner diameter of the catalytic reactor were 70 and 80 mm, respectively. The space velocity, defined as the volumetric flow rate of feed divided by the catalyst volume, was $27,300\text{ h}^{-1}$. The catalyst weight and the reaction temperature were 17.0 g and $160 \pm 20^\circ\text{C}$, respectively.

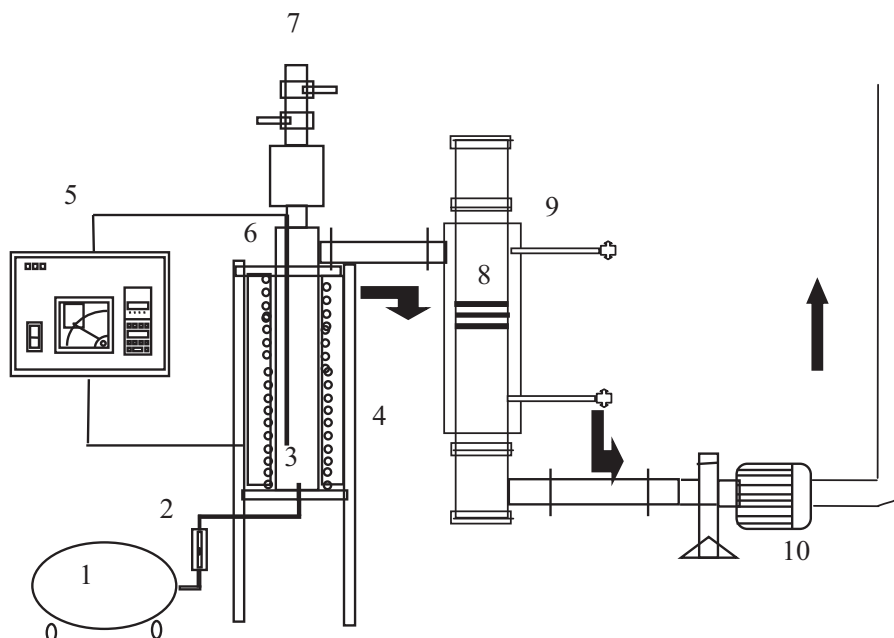


Fig. 1. Experimental system of fluidized-bed incinerator and reactor of ACFs supported catalysts. (1) Air compressor; (2) flowmeter; (3) combustion chamber; (4) electrical heater; (5) thermal feedback controller; (6) thermocouple; (7) feeder; (8) reactor of ACFs supported catalysts; (9) sampling; (10) induced fan.

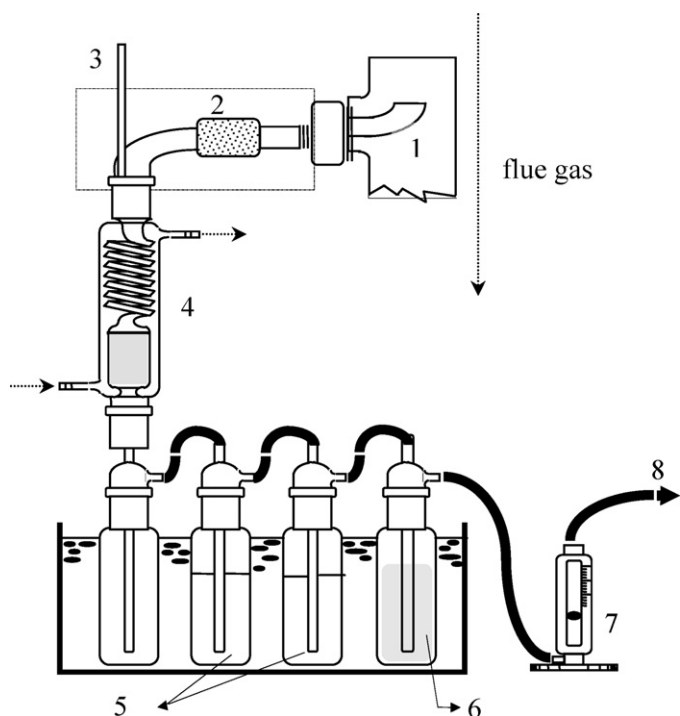


Fig. 2. Sampling train for PAHs. (1) Sampling probe; (2) heated filter and heating hose; (3) thermometer; (4) cooling tube and XAD-4 adsorption tube; (5) 200 ml distilled water; (6) silica gel; (7) flow meter; (8) connect to vacuum pump.

Silica sand (200 g) was used for the fluidized-bed material and the temperature of the sand bed was determined by a thermocouple. The combustion chamber was heated to the desired temperature (800 °C) by electrical heaters. Room-temperature air was introduced at 60 L/min with an excess air ratio of 50%. When the air temperature reached a steady state, the artificial feedstock was fed into the incinerator at the rate of one bag every 15 s. Subsequently, the combustion gases were treated in the catalytic reactor, and then released into the atmosphere. The experiment was performed continuously until the sampling tasks were completed.

2.4. Sampling and analytical methods

The flue gas, containing fly ash and PAHs, was simultaneously sampled by the USEPA modified method 5 (MM5) both prior to and after passing through the catalytic reactor. To avoid the fluctuation of PAHs concentration over time, the sampling time and period of each test were the same. The sampling time of each test, after and before the passage of the flue gas through the catalytic reactor were at 5–15 min and 20–30 min after the catalytic reactor was turned on, respectively. The sampling period of each test was 10 min. The removal efficiencies of PAHs were defined as $\%PAHs = [(PAHs_{inlet} - PAHs_{outlet}) \times 100] / PAHs_{inlet}$. Fig. 2 shows the sampling train. The gas passed through a heated filter packed with fiberglass to collect particles and then through a cooling tube to capture the remaining PAHs on XAD-2 adsorbent. Next, the sampled materials, including particles and XAD-2 adsorbent, were extracted over 20 h using the Soxhlet extraction process. The extraction solution was concentrated to 1 ml using a KD evaporator concentrator. These samples were then analyzed using a gas chromatograph with a flame ionization detector (Shimadzu GC-2014). The R^2 of all calibration curves are above 0.99 and the concentration of all extraction solutions are above the detection limit of GC.

2.5. Catalysts characterization

The Brunauer–Emmett–Teller (BET) surface area and the Barrett–Joyner–Halenda (BJH) pore volume of various ACFs were determined using an ASAP 2010 vacuum volumetric sorption instrument from the N_2 adsorption–desorption isotherms at 77 K. Before N_2 sorption analysis, the samples were degassed at 220 °C for 24 h and cooled at room temperature under vacuum. The mesopore volumes of various ACFs were determined using the BJH method. The volume of micropores was calculated using the t -plot method. The ACFs were pretreated by microwave digestion (CEM MARS), and then the digestion liquid was analyzed by inductively coupled plasma (ICP; Optima 2100DV, Perkin Elmer) to estimate the metal loading in the ACFs. The standard addition method was employed, and a recovery efficiency of $100 \pm 15\%$ was obtained. A micrograph of the ACFs was obtained using a field-emission scanning electron microscopy (FE-SEM; Model JSM-6700F, JEOL, Tokyo, Japan) operated at 5 kV and equipped with an X-ray energy-dispersive spectrometer (EDS).

The metal species on the ACFs were identified by an X-ray powder diffractometer (SIEMENS D5000) equipped with a $Cu K\alpha$ radiation source ($\lambda = 1.5418 \text{ \AA}$). The powdered samples were pressed onto suitable holders and were scanned within the 2θ angle range $10\text{--}90^\circ$, in steps of 0.04° . The scanning speed was 4° min^{-1} . To obtain information about the metal oxidation state, the X-ray photoelectron spectroscopy (XPS) examination for the catalysts were carried out using a VG Scientific ESCALAB 250 spectrometer with $Al K\alpha$ X-ray (1486.6 eV).

A Fourier-transform infrared spectrometer (FTIR; DIGILAB FTX350, American DIGILAB) was used to identify the surface functional groups on the ACFs. The infrared spectra of the ACFs were recorded in the range between 800 and 4000 cm^{-1} . The FTIR analysis was performed after grinding the ACFs and mixing with KBr powder to prepare sample-KBr pellets. Before the spectra were recorded, these pellets were dried in the oven at 105 °C for 12 h. The ACFs were mixed with KBr at an approximate ratio of 1/99.

3. Results and discussion

3.1. Characterization of ACF-supported metal catalysts

3.1.1. BET surface area measurement

The BET surface area and porous structure of the ACFs is summarized in Table 2. The results show that the order of the BET surface area of the Pd based catalysts is original ACFs > 0.11% Pd/ACFs > 0.29% Pd/ACFs > 0.34% Pd/ACFs. The reduction of surface area indicated here might be due to the filling of the ACF pores with the metal particles. The above conjecture can be confirmed from the total pore volumes in Table 2. Comparatively, the BET surface area and the mesopore volume of the Pd based catalysts increased significantly after the ACFs were pretreated with HNO_3 and NaOH. A possible explanation is that the inorganic substances on the ACFs were removed.

3.1.2. XRD analysis

The X-ray diffraction patterns of the fresh catalysts are shown in Fig. 3. It was observed that only graphite crystallite was present in the catalysts ($2\theta = 24\text{--}26^\circ$ and 43.3°). The loss of intensity in the 1.63% Pt/ACFs may be due to the higher loading of metal over the 1.63% Pt/ACFs or the effects of $PtCl_4$ precursor. Previous studies have reported that the reflections of lower metal loadings on relatively high surface area supports were hardly observed because of their highly dispersed surface phase [6,20–23]. We therefore suggest, from our results, that the metal particles were well dispersed on the ACFs.

Table 2
BET surface area, micropore and mesopore volume of ACFs by N₂ isotherms.

Catalyst	S_{BET}^a (m ² /g)	V_T^b (cm ³ /g)	t-Plot method		V_{meso} (2–50 nm) (cm ³ /g)
			S_{micro}^c (<2 nm) (m ² /g)	V_{micro} (<2 nm) (cm ³ /g)	
Original ACFs	1235	0.607	577	0.253	0.354
0.11% Pd/ACFs	1193	0.564	678	0.290	0.274
0.29% Pd/ACFs	1189	0.567	632	0.270	0.297
0.34% Pd/ACFs	1154	0.554	644	0.265	0.289
1.63% Pt/ACFs	1102	0.514	657	0.275	0.239
0.53% Cu/ACFs	1045	0.498	681	0.298	0.200
HNO ₃ -0.48% Pd/ACFs	1444	0.715	646	0.265	0.451
NaOH-0.52% Pd/ACFs	1230	0.607	500	0.203	0.404
Spent original ACFs	1054	0.553	545	0.294	0.259
Spent 0.34% Pd/ACFs	885	0.463	489	0.263	0.200
Spent HNO ₃ -0.48% Pd/ACFs	993	0.524	343	0.190	0.334
Spent NaOH-0.52% Pd/ACFs	880	0.462	547	0.291	0.171

^a Specific surface area by BET method.

^b Total pore volume, $V_T = V_{\text{micro}} + V_{\text{meso}}$.

^c Micropore surface area.

3.1.3. XPS analysis

The binding energy of Pd (3d_{5/2}) for 0.34% Pd/ACFs shown in Fig. 4(a) was 337.7 eV, which can be assigned to PdO₂/Pd⁴⁺. The peak at 73.3 eV shown in Fig. 4(b) represents the characteristic of oxidized state (PtO₂/Pt⁴⁺) of 1.63% Pt/ACFs [24]. These results

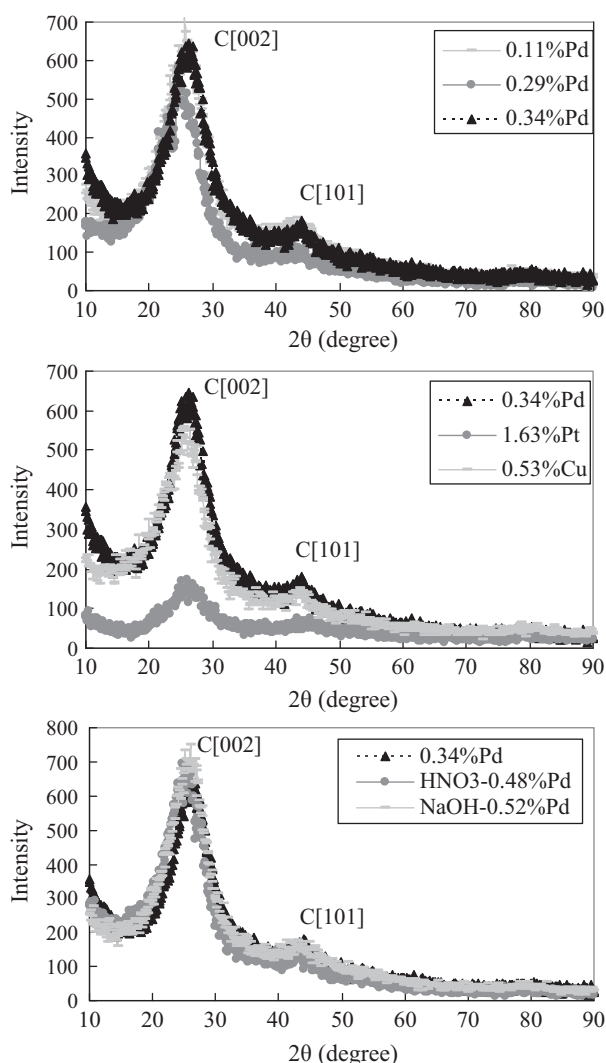


Fig. 3. XRD spectra of various catalysts.

confirm the existence of the oxidized metal phases onto the ACFs-supported the catalysts.

3.1.4. FTIR analysis

Fig. 5 shows the FTIR spectra of the fresh catalysts of 0.34% Pd/ACFs, HNO₃-0.48% Pd/ACFs, and NaOH-0.52% Pd/ACFs. In the FTIR spectra of HNO₃-0.48% Pd/ACFs and NaOH-0.52% Pd/ACFs, faint new bands appear between 1400 and 2000 cm⁻¹. It has been reported that bands at 1100–1450 cm⁻¹ could be related to C–O stretching. Peaks at 1550–2050 cm⁻¹ corresponded to C=O stretching of carboxylic acid and lactone [17,25]. Previous study showed that the enhanced acid surface nature could be responsible for the improved catalytic activity [17]. In this study, the FTIR spectra in Fig. 5 can explain that the removal of PAHs was improved significantly when using the catalysts HNO₃-0.48% Pd/ACFs and NaOH-0.52% Pd/ACFs.

3.1.5. FESEM and EDS analysis

Figs. 6 and 7 show the FE-SEM micrograph and EDS images of 0.34% Pd/ACFs, HNO₃-0.48% Pd/ACFs and NaOH-0.52% Pd/ACFs.

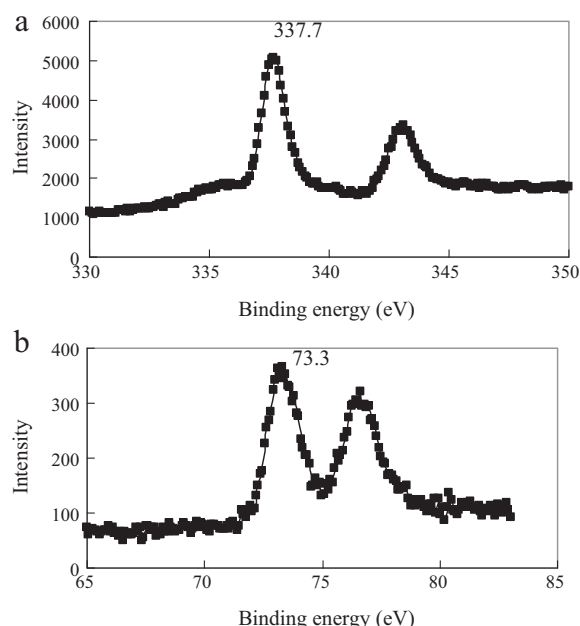


Fig. 4. XPS spectra of ACF-supported catalysts (a) 0.34% Pd/ACFs (b) 1.63% Pt/ACFs.

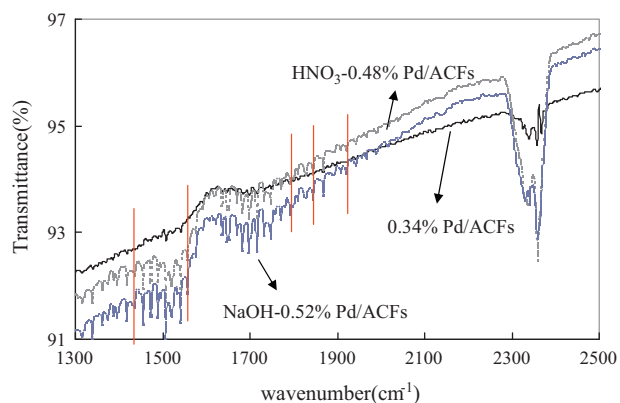


Fig. 5. FTIR spectra of 0.34% Pd/ACFs, HNO₃-0.48% Pd/ACFs and NaOH-0.52% Pd/ACFs.

Fig. 6 also confirms that the Pd particles were well dispersed on the surface of the ACFs. The presence of the Pd element was also determined by SEM-EDS, as shown in Fig. 7.

3.2. Removal of PAHs

3.2.1. Effect of Pd loading

Fig. 8 shows the effects of Pd loading on PAHs removal. The results indicate that the removal of PAHs was improved slightly using Pd catalysts supported on ACFs. For the Pd/ACFs catalysts with different Pd loadings, the PAHs removal follows the order: 0.29% Pd/ACFs > 0.34% Pd/ACFs > 0.11% Pd/ACFs. Table 1 shows that the measured metal loadings of the three catalysts, 0.11% Pd/ACFs, 0.29% Pd/ACFs and 0.34% Pd/ACFs, were 0.11 wt%, 0.29 wt% and 0.34 wt%, respectively. Moreover, Table 2 shows that the mesopore

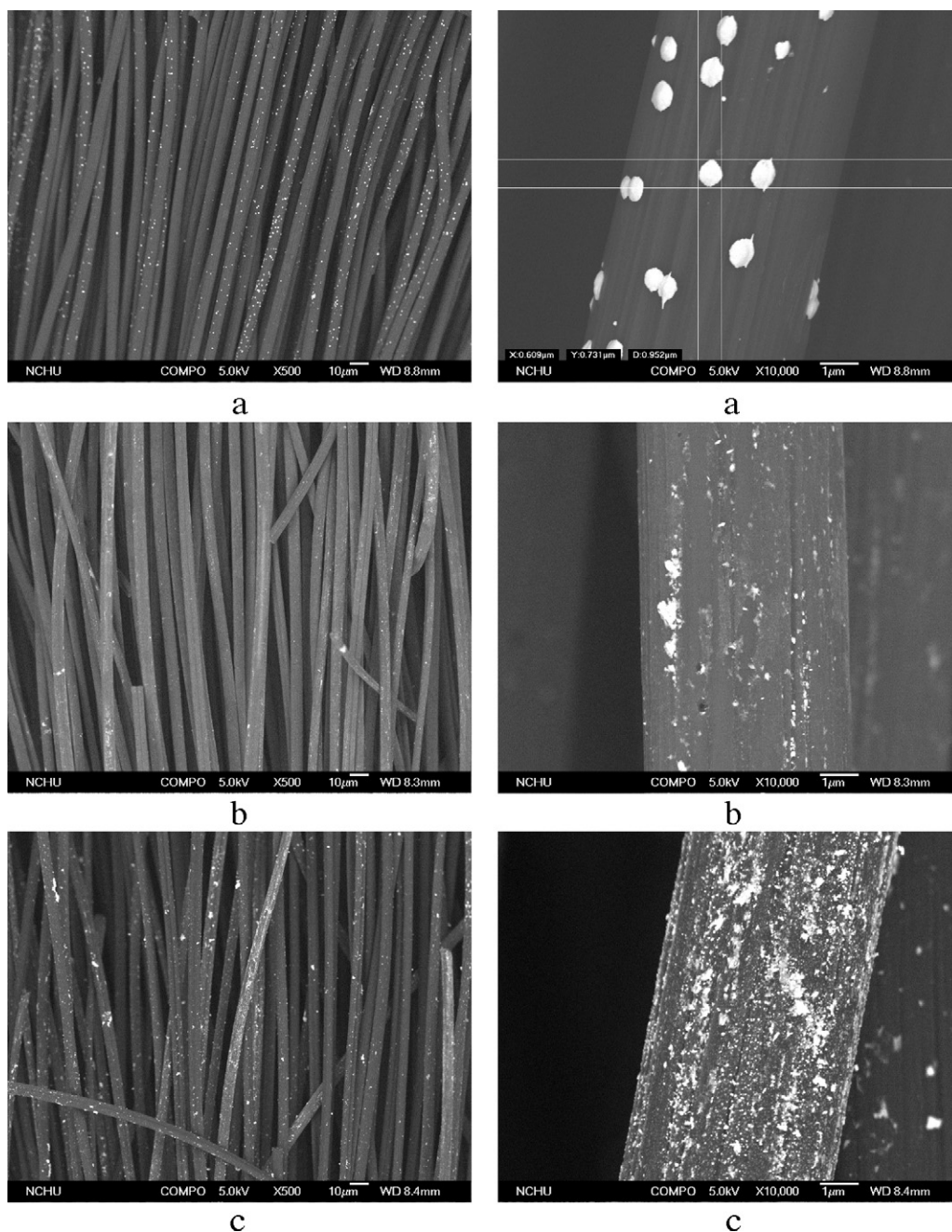


Fig. 6. FESEM micrograph of the catalysts: (a) 0.34% Pd/ACFs (b) HNO₃-0.48% Pd/ACFs (c) NaOH-0.52% Pd/ACFs.

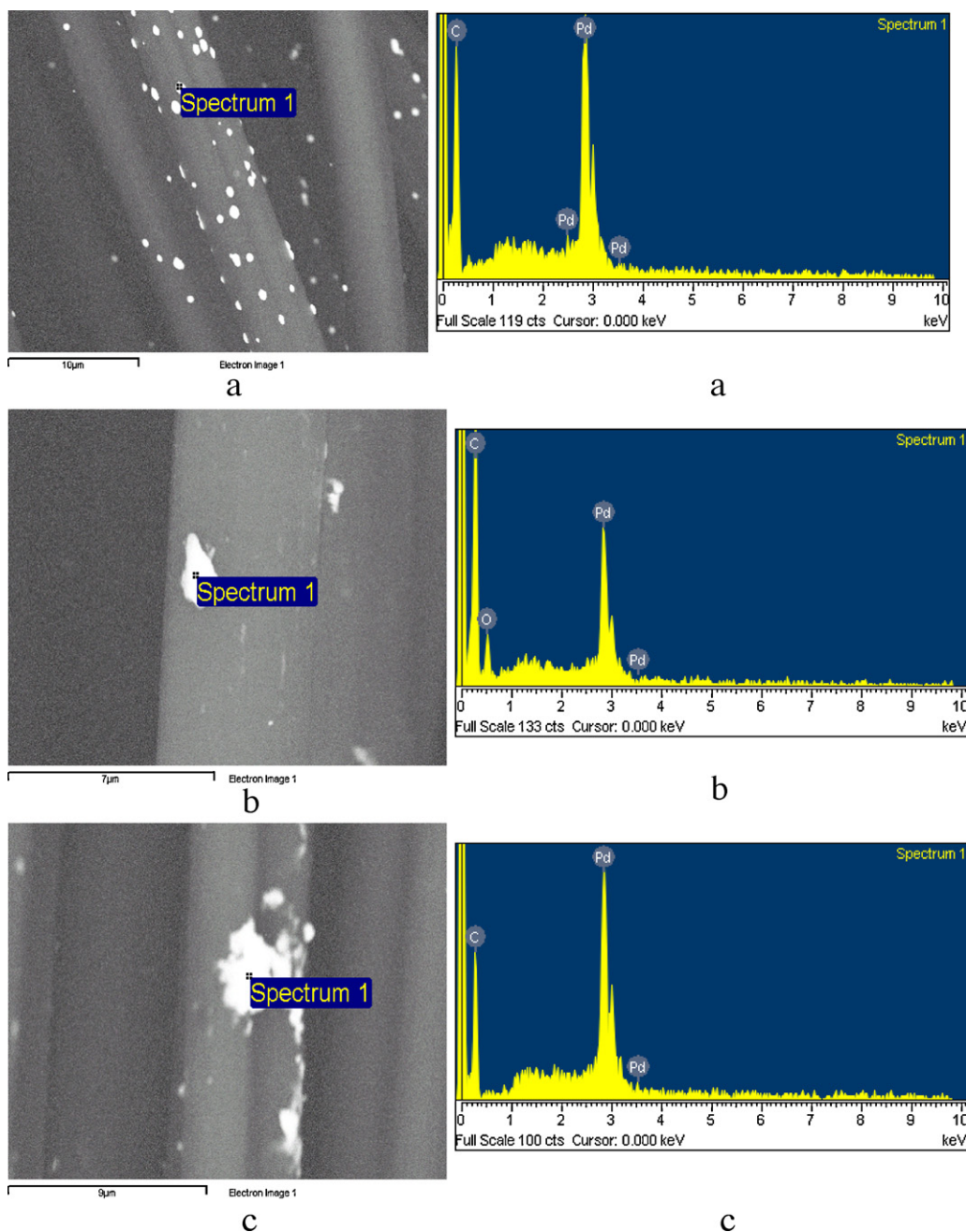


Fig. 7. SEM-EDS image of the catalysts: (a) 0.34% Pd/ACFs (b) HNO_3 -0.48% Pd/ACFs (c) NaOH -0.52% Pd/ACFs.

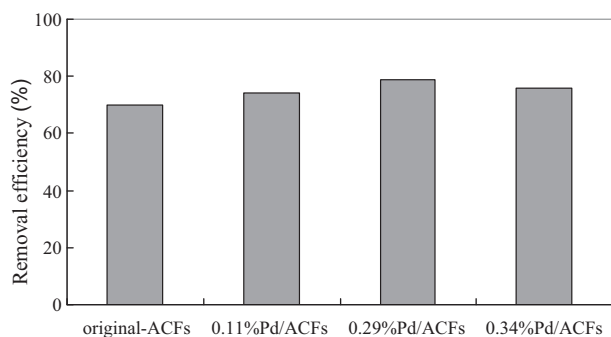


Fig. 8. Effects of Pd loading on PAHs removal.

volume of 0.11% Pd/ACFs, 0.29% Pd/ACFs and 0.34% Pd/ACFs were 0.2738 cm³/g, 0.2966 cm³/g and 0.2886 cm³/g, respectively. The order of the PAHs removal of three Pd loadings is in accordance with the mesopore volume of the ACFs catalysts. As a result, when the difference in Pd loading between the ACFs catalysts was unapparent, the mesopore volume played an important role in determining the PAHs removal was supposed in this study.

Previous studies have shown that the molecules adsorbed on activated carbon would proceed through a sequence of diffusion steps from the bulk phase into the mesopores and then to the micropores. These micropores cannot be completely utilized in adsorption and the fractional coverage of these micropores may depend on the length of the diffusion path. A longer diffusion path will result in a greater probability for the pore blockage to occur. Therefore, with the existence of mesopores in activated carbon, the diffusion path from mesopores to the carbon interior will be shorter

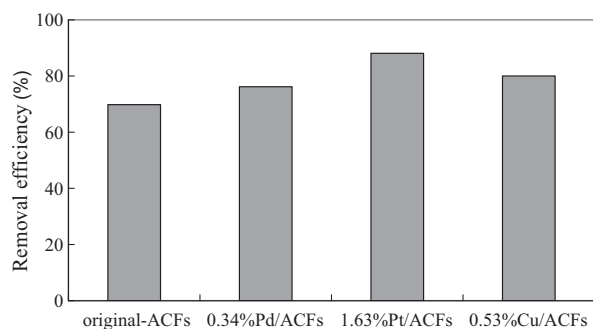


Fig. 9. Effects of three metal catalysts on PAHs removal.

than that when the diffusion comes directly from the bulk phase to the carbon interior without the aid of mesopores [26,27]. The highest PAHs removal of 0.29% Pd/ACFs can be explained by the fact that the 0.29% Pd/ACFs contains higher mesopore volume (Table 2), thus shortening the diffusion path for PAHs to get access to the ACFs interior. The existence of mesopores in ACFs is important in enhancing the PAHs removal, especially for the larger molecules.

3.2.2. Effects of three metal catalysts

Fig. 9 illustrates the effects of three metal catalysts on the removal of PAHs. The results reveal that the order of removal is 1.63% Pt/ACFs > 0.53% Cu/ACFs > 0.34% Pd/ACFs > original ACFs. Previous studies have reported that platinum is the most active metal for oxidation of all the hydrocarbons except methane [28]. Table 2 shows the BET surface area and porosity of ACFs. From this it seems that efficacy of PAH removal is not associated with the specific surface area of the ACFs. Our earlier study demonstrated that the BET surface area did not affect the removal of PAHs when the concentration of PAHs (in relation to ACFs) was low and the BET surface area was sufficient to support PAHs removal [2]. In the present experiment, the measured metal loadings of the three catalysts, 0.34% Pd/ACFs, 1.63% Pt/ACFs, and 0.53% Cu/ACFs, were 0.34 wt%, 1.63 wt% and 0.53 wt%, respectively (see Table 1). Our results suggest that Pt was more easily adsorbed on ACFs than Pd or Cu.

3.2.3. Effects of pretreatment solutions

The mesopore volumes of the ACFs increased significantly after treating with HNO₃ and NaOH solutions (Table 2). The FTIR spectra shown in Fig. 5 indicate that new functional groups were observed in HNO₃-0.48% Pd/ACFs and NaOH-0.52% Pd/ACFs. These results explain why the measured metal loading in HNO₃-0.48% Pd/ACFs and NaOH-0.52% Pd/ACFs was higher than that in 0.34% Pd/ACFs (Table 1).

Fig. 10 illustrates the effects of the pretreatment solutions. The data indicate that the removal of PAHs was improved significantly when using the catalysts HNO₃-0.48% Pd/ACFs and NaOH-0.52%

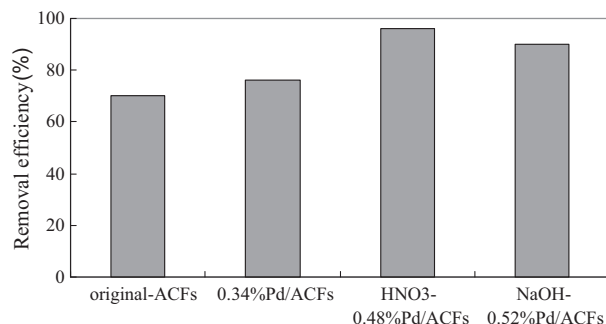


Fig. 10. Effects of pretreatment solution on PAHs removal.

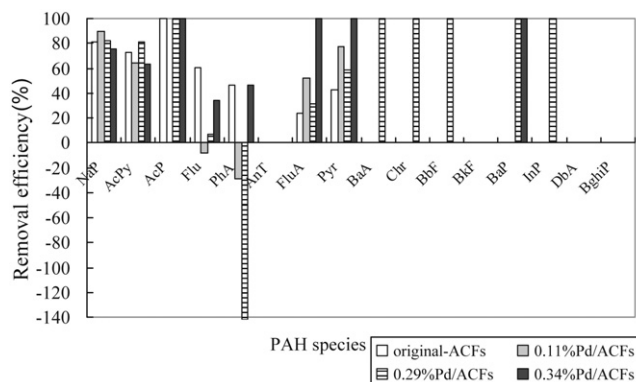


Fig. 11. Effects of Pd loading on removal efficiency of sixteen species of PAHs.

Pd/ACFs. The FE-SEM micrograph and SEM-EDS image shown in Figs. 6 and 7 illustrate that lower Pd dispersion and the formation of bigger Pd agglomerates in HNO₃-0.48% Pd/ACFs and NaOH-0.52% Pd/ACFs. These results are in agreement with previous studies, which reported that high-activity catalysts for naphthalene oxidation required a lower Pt dispersion and a larger-than-average active Pt particle size [28,29]. This relates to the fact that naphthalene is a relatively large molecule compared with many of the reactants previously investigated on Pt-based catalysts and a larger particle size is required for adsorption and oxidation to take place [29].

3.3. Effective removal of 16 species of PAHs

Figs. 11–13 show the effects of Pd loading, the use of three metal catalysts and pretreatment solution, respectively, on the efficient removal of 16 species of PAHs. The results indicate that the removal efficiencies of the higher-ring compounds (such as BaA, Chr, BbF, BkF, BaP, InP, and BghiP) can be improved significantly by the ACFs-supported metal catalysts. In this study, the BET surface area and the pore volume of four spent catalysts (original ACFs, 0.34% Pd/ACFs, HNO₃-0.48% Pd/ACFs and NaOH-0.52% Pd/ACFs) were also analyzed by an ASAP 2010 instrument. Table 2 shows that the BET surface area and the mesopore volume of four spent catalysts decreased significantly. This can confirm that 16 PAH species mainly adsorbed onto the mesopores. Moreover, Table 3 lists the physical and chemical properties of the 16 PAH species. Table 3 demonstrates that the molecular size of lower-ring compounds (two- and three-benzene rings) is smaller than that of higher-ring compounds (four-, five-, and six-benzene rings), and Tables 4 and 5 show that the concentration of lower-ring compounds in the incineration flue gas is much higher than that of higher-ring compounds.

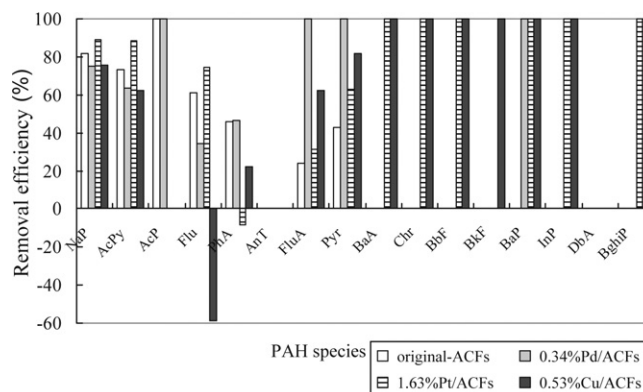
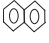
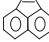
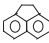
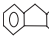
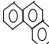
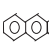

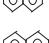
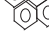
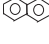
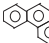
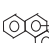
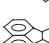
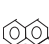
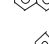
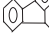


Fig. 12. Effects of three metal catalysts on removal efficiency of sixteen species of PAHs.

Table 3
The physical and chemical properties of PAHs [1,30].

Compound	Abbreviation	Chemical formula	Width (Å)	Length (Å)	Thickness (Å)	Molecular weight	Melting point (°C)	Boiling point (°C)	Vapor pressure (mmHg, 25 °C)	Structure
Naphthalene	NaP	C ₁₀ H ₈	7.428	9.195	3.884	128.16	80	218	7.1 × 10 ⁻²	
Acenaphthylene	AcPy	C ₁₂ H ₈	8.488	9.238	4.221	152.20	93	275	6.7 × 10 ⁻³	
Acenaphthene	AcP	C ₁₂ H ₁₀	8.624	9.242	3.882	154.21	96	279	2.2 × 10 ⁻³	
Fluorene	Flu	C ₁₃ H ₁₀	7.521	11.431	4.241	166.22	117	295	6.0 × 10 ⁻⁴	
Phenanthrene	PhA	C ₁₄ H ₁₀	8.031	11.752	3.888	178.22	100	340	1.2 × 10 ⁻⁴	
Anthracene	AnT	C ₁₄ H ₁₀	7.439	11.651	3.882	178.22	218	342	6.0 × 10 ⁻⁶	
Fluoranthene	FluA	C ₁₆ H ₁₀	9.240	11.158	3.884	202.26	110	393	9.2 × 10 ⁻⁶	
Pyrene	Pyr	C ₁₆ H ₁₀	9.279	11.662	3.888	202.26	156	404	4.5 × 10 ⁻⁶	
Benzo(a)anthracene	BaA	C ₁₈ H ₁₂	8.717	13.942	3.887	228.29	159	435	2.1 × 10 ⁻⁷	
Chrysene	Chr	C ₁₈ H ₁₂	8.039	13.939	3.922	228.29	256	448	6.4 × 10 ⁻⁹	
Benzo(b)fluoranthene	BbF	C ₂₀ H ₁₂	9.964	13.817	3.884	252.32	168	393	–	
Benzo(k)fluoranthene	BkF	C ₂₀ H ₁₂	9.242	13.618	3.887	252.32	217	480	9.6 × 10 ⁻¹¹	
Benzo(a)pyrene	BaP	C ₂₀ H ₁₂	9.297	13.882	3.891	252.32	177	496	5.6 × 10 ⁻⁹	
Indeno(1,2,3-cd)pyrene	InP	C ₂₂ H ₁₂	9.927	13.780	3.884	276.34	162	534	–	
Dibenzo(a,h)anthracene	DbA	C ₂₂ H ₁₄	8.726	15.898	3.890	278.35	262	535	–	
Benzo(g,h,i)perylene	BghiP	C ₂₂ H ₁₂	10.484	11.779	3.887	276.34	273	542	1.01 × 10 ⁻¹⁰	

Thus, the probability of lower-ring PAHs proceeded into the interior of the ACFs was higher, and the amount of lower-ring PAHs adsorbed on ACFs was higher than that of higher-ring PAHs. Then, the adsorptive site would be occupied by the lower-ring PAHs.

However, when the ACFs-supported metal catalysts was used to remove 16 species of PAHs, the lower-ring PAHs adsorbed on the ACFs could be catalyzed, and then the adsorptive site of ACFs would be liberated. The probability of higher-ring PAHs adsorbed on ACFs

Table 4
Inlet and outlet PAHs concentrations and removal efficiency of 16 PAH species over ACFs-supported Pd catalyst.

Species	Original ACFs			0.11% Pd/ACFs			0.29% Pd/ACFs			0.34% Pd/ACFs		
	C _{inlet} (mg/Nm ³)	C _{outlet} (mg/Nm ³)	RE (%)	C _{inlet} (mg/Nm ³)	C _{outlet} (mg/Nm ³)	RE (%)	C _{inlet} (mg/Nm ³)	C _{outlet} (mg/Nm ³)	RE (%)	C _{inlet} (mg/Nm ³)	C _{outlet} (mg/Nm ³)	RE (%)
NaP	18.0	3.3	82	18.0	1.9	89	15.0	2.7	82	20.0	5.0	75
AcPy	1.5	0.4	73	1.0	0.4	64	2.5	0.5	81	2.5	0.9	64
AcP	1.2	0.0	100	0.0	0.0	0	0.5	0.0	100	0.0	0.0	100
Flu	0.2	0.1	61	0.1	0.1	-8	0.1	0.1	7	0.1	0.0	34
PhA	2.8	1.5	46	2.3	3.0	-29	1.0	2.4	-142	2.8	1.5	47
AnT	0.0	0.0	0	0.0	0.0	0	0.0	0.0	0	0.0	0.0	0
FluA	2.6	2.0	24	3.5	1.7	52	2.8	1.9	31	3.5	0.0	100
Pyr	2.3	1.3	43	4.5	1.0	77	3.0	1.2	59	3.0	0.0	100
BaA	0.3	0.3	0	0.0	0.0	0	3.0	0.0	100	0.0	0.0	0
Chr	0.0	0.0	0	0.0	0.0	0	3.8	0.0	100	0.0	0.0	0
BbF	0.0	0.0	0	0.0	0.0	0	3.8	0.0	100	0.0	0.0	0
BkF	0.2	0.2	0	0.0	0.0	0	0.0	0.0	0	0.5	0.5	0
BaP	0.0	0.0	0	0.0	0.0	0	2.2	0.0	100	2.2	0.0	100
InP	0.0	0.0	0	0.0	0.0	0	1.8	0.0	100	0.5	0.5	0
DbA	0.0	0.0	0	0.0	0.0	0	0.0	0.0	0	0.0	0.0	0
BghiP	0.0	0.0	0	0.0	0.0	0	0.0	0.0	0	0.5	0.5	0

Table 5
Inlet and outlet PAHs concentrations and removal efficiency of 16 PAH species over various catalysts.

Species	1.63% Pt/ACFs			0.53% Cu/ACFs			HNO ₃ -0.48% Pd/ACFs			NaOH-0.52% Pd/ACFs		
	C _{inlet} (mg/Nm ³)	C _{outlet} (mg/Nm ³)	RE (%)	C _{inlet} (mg/Nm ³)	C _{outlet} (mg/Nm ³)	RE (%)	C _{inlet} (mg/Nm ³)	C _{outlet} (mg/Nm ³)	RE (%)	C _{inlet} (mg/Nm ³)	C _{outlet} (mg/Nm ³)	RE (%)
NaP	18.0	2.0	89	16.0	3.9	76	17.0	0.8	95	20.0	0.4	98
AcPy	2.7	0.3	88	0.4	0.4	62	2.0	0.2	91	2.9	2.0	32
AcP	0.0	0.0	0	0.0	0.0	0	0.0	0.0	0	0.0	0.0	0
Flu	0.2	0.1	75	0.1	0.1	-59	0.7	0.1	86	1.0	0.0	100
PhA	1.5	1.6	-8	1.2	0.9	22	3.5	0.1	96	3.5	0.5	87
AnT	0.0	0.0	0	0.0	0.0	0	1.4	0.1	96	1.1	0.1	87
FluA	1.0	0.7	31	3.5	1.3	62	3.5	0.1	97	3.2	0.4	87
Pyr	1.0	0.4	63	3.0	0.5	82	3.5	0.1	98	3.6	0.4	89
BaA	2.5	0.0	100	1.5	0.0	100	1.1	0.0	99	0.0	0.0	0
Chr	1.5	0.0	100	0.9	0.0	100	0.9	0.0	100	1.2	0.1	89
BbF	1.5	0.0	100	0.9	0.0	100	0.9	0.0	100	1.2	0.2	86
BkF	0.0	0.0	0	0.5	0.0	100	0.3	0.0	100	0.5	0.5	0
BaP	3.5	0.0	100	3.2	0.0	100	3.0	0.0	100	3.0	0.4	87
InP	2.0	0.0	100	1.5	0.0	100	0.0	0.0	0	2.5	0.2	91
DbA	0.0	0.0	0	0.0	0.0	0	0.0	0.0	0	0.0	0.0	0
BghiP	3.5	0.0	100	0.8	0.0	100	0.0	0.0	0	3.0	0.0	100

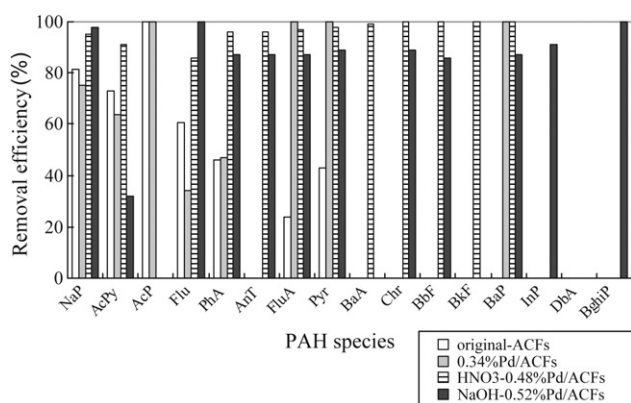


Fig. 13. Effects of pretreatment solution on removal efficiency of sixteen species of PAHs.

could increase during the catalysis process. As a result, the ACFs-supported metal catalysts could improve significantly the removal efficiencies of the higher-ring PAHs.

Figs. 11 and 12 illustrate that the removal efficiency of three-ring PAHs (such as Flu and PhA) are negative using 0.11% Pd/ACFs, 0.29% Pd/ACFs, 1.63% Pt/ACFs and 0.53% Cu/ACFs. The result can be explained by the fact that the Flu and PhA might be the major oxidation byproducts during catalysis. Diehl et al. investigated the catalytic oxidation of heavy hydrocarbons over Pt/Al₂O₃ [28]. They found that the catalytic oxidation of fluorene was quite different from that of other hydrocarbons. Detailed analysis showed that fluorenone was the major oxidation product even at very high fluorene conversion. Thus, the higher outlet concentrations of Flu and PhA were found in this research. It is necessary to analyze the outlet concentrations of all the byproducts in detail to understand their reactivity for heavy aromatics.

4. Conclusions

The adsorption and catalytic oxidation of 16 polycyclic aromatic hydrocarbons (PAHs) in incineration flue gas by ACF-supported metal catalysts were investigated in this study. Experimental results showed that the order of removal of the PAHs for three metal loadings was 0.29% Pd/ACFs > 0.34% Pd/ACFs > 0.11% Pd/ACFs > original ACFs. The order of the PAHs removal of three Pd loadings was in accordance with the mesopore volume of the ACFs catalysts. Our results also suggest that Pt was more easily

adsorbed on ACFs than Pd and Cu, and Pt was the most active metal in oxidation of the PAHs. The mesopore volumes and density of new functional groups on the ACFs increased significantly after treating with HNO₃ and NaOH solutions, and led to increase metal loadings in HNO₃-0.48% Pd/ACFs and NaOH-0.52% Pd/ACFs. These data confirmed improved PAHs removal with HNO₃-0.48% Pd/ACFs and NaOH-0.52% Pd/ACFs. Moreover, the ACFs-supported metal catalysts could improve significantly the removal efficiencies of the higher-ring PAHs (such as BaA, Chr, BbF, BkF, BaP, InP, and BghiP). However, future research will need to make a detailed analysis of all the byproducts of the sixteen species of PAHs to understand their reactivity more fully.

Acknowledgments

The writer would like to thank the National Science Council of the Republic of China, Taiwan for financially supporting this research under Contract No. NSC 96-2221-E-131-019-MY3.

References

- [1] Z.S. Liu, M.Y. Wey, C.L. Lin, Simultaneous control of acid gases and PAHs using a spray dryer integrated with a fabric filter using different additives, *J. Hazard. Mater.* B91 (2002) 129–141.
- [2] Z.S. Liu, Control of PAHs from incineration by activated carbon fibers, *J. Environ. Eng. ASCE* 132 (2006) 463–469.
- [3] J.L. Shie, C.Y. Chang, J.H. Chen, W.T. Tsai, Y.H. Chen, C.S. Chiou, C.F. Chang, Catalytic oxidation of naphthalene using a Pt/Al₂O₃ catalyst, *Appl. Catal. B: Environ.* 58 (2005) 289–297.
- [4] W.G. Shim, S.C. Kim, H.C. Kang, S.W. Nahm, J.W. Lee, H. Moon, Influence of pretreatment methods on adsorption and catalytic characteristics of toluene over heterogeneous palladium based catalysts, *Appl. Surf. Sci.* 253 (2007) 5868–5875.
- [5] M. Guillelot, J. Mijoin, S. Mignard, P. Magnoux, Volatile organic compounds (VOCs) removal over dual functional adsorbent/catalysts system, *Appl. Catal. B: Environ.* 75 (2007) 249–255.
- [6] J.C.S. Wu, Z.A. Lin, F.M. Tsai, J.W. Pan, Low temperature complete oxidation of BTX on Pt/activated carbon catalysts, *Catal. Today* 63 (2000) 419–426.
- [7] F.Y. Yi, X.D. Lin, S.X. Chen, X.Q. Wei, Adsorption of VOC on modified activated carbon fiber, *J. Porous Mater.* 16 (2008) 521–526.
- [8] H.T. Zeng, Y. Li, S. Chen, P.K. Shen, Effect of support on the activity of Pd electrocatalyst for ethanol oxidation, *J. Power Sources* 163 (2006) 371–375.
- [9] H.X. Huang, S.X. Chen, C. Yuan, Platinum nanoparticles supported on activated carbon fiber as catalyst for methanol oxidation, *J. Power Sources* 175 (2008) 166–174.
- [10] J.B. Donnet, R.C. Bansal, F. Stoeckli, *Carbon Fibers*, Marcel Dekker, New York, 1990.
- [11] R.N. McNair, G.N. Arons, *Sorptive Textile Systems Containing Active Carbon Fibers*, Carbon Adsorption Handbook (Chapter 22), Ann Arbor Science, MI, 1980, p. 819.
- [12] P. Gélin, M. Primet, Complete oxidation of methane at low temperature over noble metal based catalysts: a review, *Appl. Catal. B: Environ.* 39 (2002) 1–37.

- [13] M.R. Morales, B.P. Barbero, L.E. Cadús, Combustion of volatile organic compounds on manganese iron or nickel mixed oxide catalysts, *Appl. Catal. B: Environ.* 74 (2007) 1–10.
- [14] S.C. Kim, The catalytic oxidation of aromatic hydrocarbons over supported metal oxide, *J. Hazard. Mater.* B91 (2002) 285–299.
- [15] C.H. Wang, S.S. Lin, C.L. Chen, H.S. Weng, Performance of the supported copper oxide catalysts for the catalytic incineration of aromatic hydrocarbons, *Chemosphere* 64 (2006) 503–509.
- [16] D.A. Bulushev, I. Yuranov, E.I. Suvorova, P.A. Buffat, L. Kiwi-Minsker, Highly dispersed gold on activated carbon fibers for low-temperature CO oxidation, *J. Catal.* 224 (2004) 8–17.
- [17] S. Hermans, C. Diverchy, O. Demoulin, V. Dubois, E.M. Gaigneaux, M. Devillers, Nanostructured Pd/C catalysts prepared by grafting of model carboxylate complexes onto functionalized carbon, *J. Catal.* 243 (2006) 239–251.
- [18] V.Z. Radkevich, T.L. Senko, K. Wilson, L.M. Grishenko, A.N. Zaderko, V.Y. Diyuk, The influence of surface functionalization of activated carbon on palladium dispersion and catalytic activity in hydrogen oxidation, *Appl. Catal. A: Gen.* 335 (2008) 241–251.
- [19] Z.S. Liu, Adsorption of SO₂ and NO from incineration flue gas onto activated carbon fibers, *Waste Manage.* 28 (2008) 2329–2335.
- [20] J. Batista, A. Pintar, J.P. Gomilsek, A. Kodre, F. Bornette, On the structural characteristics of γ -alumina-support Pd–Cu bimetallic catalysts, *Appl. Catal. A: Gen.* 217 (2001) 55–68.
- [21] X.W. Zhang, S.C. Shen, L.E. Yu, S. Kawi, K. Hidajat, K.Y.S. Na, Oxidative decomposition of naphthalene by supported metal catalysts, *Appl. Catal. A: Gen.* 250 (2003) 341–352.
- [22] H.S. Kim, T.W. Kim, H.L. Koh, S.H. Lee, B.R. Min, Complete benzene oxidation over Pt–Pd bimetal supported on γ -alumina: influence of Pt–Pd ration on the catalytic activity, *Appl. Catal. A: Gen.* 280 (2005) 125–131.
- [23] S.C. Kim, S.W. Nahm, W.G. Shim, J.W. Lee, H. Moon, Influence of physicochemical treatments on spent palladium based catalyst for catalytic oxidation of VOCs, *J. Hazard. Mater.* 141 (2007) 305–314.
- [24] <http://www.lasurface.com/database/elementxps.php>.
- [25] P. Yang, Y. Cao, W.L. Dai, J.F. Deng, K.N. Fan, Effect of chemical treatment of activated carbon as a support for promoted dimethyl carbonate synthesis by vapor phase oxidative carbonylation of methanol over Wacker-type catalysts, *Appl. Catal. A: Gen.* 243 (2003) 323–331.
- [26] H. Teng, C.T. Hsieh, Influence of surface properties on liquid-phase adsorption of phenol by activated carbons prepared from a bituminous coal, *Ind. Eng. Chem. Res.* 37 (1998) 3618–3624.
- [27] C.T. Hsieh, H. Teng, Influence of mesopores volume and adsorbate size on adsorption capacities of activated carbons in aqueous solutions, *Carbon* 38 (2000) 863–869.
- [28] F. Diehl Jr., J. Barbier, D. Duprez, I. Guibard, G. Mabilon, Catalytic oxidation of heavy hydrocarbons over Pt/Al₂O₃: influence of the structure of the molecule on its reactivity, *Appl. Catal. B: Environ.* 95 (2010) 217–227.
- [29] N.E. Ntainjua, A.F. Carley, S.H. Taylor, The role of support on the performance of platinum-based catalysts for the total oxidation of polycyclic aromatic hydrocarbons, *Catal. Today* 137 (2008) 362–366.
- [30] W.J. Huang, *Test Methods for Air Pollutants*, ROC EPA, 1998, p.A412.70A.